

# Application of empirical and semi-analytical algorithms to MERIS data for estimating chlorophyll *a* in Case 2 waters of Lake Erie

Khalid Ali · Donna Witter · Joseph Ortiz

Received: 19 December 2012 / Accepted: 20 September 2013  
© Springer-Verlag Berlin Heidelberg 2013

**Abstract** Lake Erie is biologically the most active lake among the Great Lakes of North America, experiencing seasonal harmful algal blooms (HABs). The early detection of HABs in the Western Basin of Lake Erie (WBLE) requires a more efficient and accurate monitoring tool. Remote sensing is an efficient tool with high spatial and temporal coverage that can allow accurate and timely detection of the HABs. The WBLE is heavily influenced by the surrounding terrestrial ecosystem via rivers such as the Sandusky River and the Maumee River. As a result, the optical properties of the WBLE are influenced by multiple color producing agents (CPAs) such as phytoplankton, colored dissolved organic matter (CDOM), organic detritus, and terrigenous inorganic particles. The diversity of the CPAs and their non-linear interactions makes these waters optically complex, and the task of optical remote sensing for retrieving estimates of CPAs more challenging. Chlorophyll *a*, which is the primary light harvesting pigment in all phytoplankton, is used as a proxy for algal biomass. In this study, several published remote sensing algorithms and band ratio models were applied to the reflectance data from the full resolution MERIS sensor to remotely estimate chlorophyll *a* concentrations in the WBLE. Efficiency of the sensor and the algorithms performance were tested through a least squares regression and residual analysis. The results indicate that, among the suite of existing bio-optical models, the Simis semi-analytical algorithm

provided the best model results for measures of algal biomass in the optically complex WBLE with  $R^2$  of 0.65, RMSE 0.85  $\mu\text{g/l}$ , ( $n = 71$ ,  $P < 0.05$ ). The superior results of this model in detecting chlorophyll *a* are attributed to several factors including optimizing spectral regions that are less sensitive to CDOM and the incorporation of correction factors such as absorption effects due to pure water ( $a_w$ ), backscatter ( $b_b$ ) from suspended matter and interference due to phycocyanin ( $\delta$ ), a major accessory pigment in the WBLE.

**Keywords** Remote sensing · Algal blooms · Water quality · Band ratios

## Introduction

Estimation of plant biomass in aquatic and marine systems by retrieval of chlorophyll *a* from remote sensing observations has become routine in Case 1 waters where chlorophyll *a* is the dominant color producing agent (CPA) present in the water column, and some consensus is being reached with regards to an appropriate universal algorithm (McClain 2009; Arnone et al. 2006; Gordon and Morel 1983; O'Reilly et al. 1998). Many of these relationships make use of the blue-green spectral region (Babin et al. 2003). The situation is more complex in turbid Case 2 waters where multiple CPAs may confound the reflectance signal (Morel and Prieur 1977; Mobley 1994; Wang et al. 2009). Bodies of water that are classified as Case 2 include coastal waters with significant inputs of suspended sediment and terrestrial organic matter, and shallow, highly stratified systems in which the distribution of phytoplankton may include or be dominated by blue-green algae or other algal taxa which contain accessory pigments that alter

K. Ali (✉)  
Department of Geology and Environmental Geosciences,  
College of Charleston, Charleston, SC 29424, USA  
e-mail: alika@cofc.edu

D. Witter · J. Ortiz  
Department of Geology, Kent State University, Kent,  
OH 44242, USA

the ratio of water-leaving radiances at various wavelengths. Many highly productive systems also have high concentrations of colored dissolved organic matter (CDOM), degradation products produced by the senescence and death of phytoplankton or excreted by their predators after feeding. The situation is further complicated by time-dependent changes in the concentrations of these sources of bias in these dynamic environments.

The Western Basin of Lake Erie (WBLE) qualifies as body that exhibits all of these complicating factors. Productivity is among the highest seen in fresh water ecosystems, the maximum depth of the WBLE is only 11 meters, and rivers draining eight major watersheds deliver a mix of sediment, CDOM, and riverine algae to the region. Nutrient controls in Lake Erie led to significant reduction in the biomass density in the 1980s; however, in addition to the historical issues with Lake Erie water quality, in recent years, the WBLE has experienced an increase in harmful blooms of *Microcystis aeruginosa*, a toxic blue-green alga (Ouellette et al. 2006; NOAA 2011). It is essential to efficiently and accurately monitor changes in water quality; this region of the lake serves as an economic and social resource through the fishing and recreation industries, as well as the contribution of the lake to the drinking water supply.

While the most direct methods of monitoring water quality involve the analysis of water samples, these methods do not provide the spatial and temporal coverage needed to continuously assess water quality on basin-wide scales. Use of satellite remote sensing provides complementary information which has the potential to greatly improve understanding of variations in water quality. Satellite sensors that detect variations in spectral reflectance from the Earth's surface in carefully selected bands of the visible spectrum have proven promising for water quality assessment in other locations. With these systems, assessment of water quality is obtained by applying algorithms that relate satellite-measured reflectance to the concentrations of specific CPAs (Martin 2004). Ground-truthing is achieved by comparing co-located satellite and in situ observations.

Various empirical and semi-analytical algorithms have been developed for estimating chlorophyll *a* in coastal waters (Witter et al. 2009; Gitelson et al. 2000; Schalles 2006; Dall'Olmo and Gitelson 2005; Doerffer and Schiller 2007; Moses et al. 2009; Gons 1999; Gower et al. 1999; Doerffer and Fischer 1994; Dekker et al. 1997; Dekker 1993; Gons et al. 2002; Matthews et al. 2010); however, universally applicable remote sensing algorithms for the retrieval of water constituents from Case 2 waters are not known (Arnone et al. 2006). The challenge in algorithm development in these waters comes with the overlapping magnitude of the spectral coefficients from the various

CPAs and their non-linear interaction. Moreover, the complex interactions of the physical, chemical and biological process at local environments and the lack of knowledge of the bio-optical properties specific to the region results in inaccuracies and poor performance in the standard algorithms (Woodruff et al. 1999; Whitlock et al. 1981; Wong et al. 2008). Specific algorithms are thus optimized and validated due to the optical convolution observed in turbid waters coupled with complexities of satellite observations (e.g., atmospheric interferences or issues pertaining to spatial and temporal sampling) (Gitelson et al. 2007).

Recent works demonstrated that applying standard bio-optical models to the WBLE has proven challenging due to the difficulty of separating the spectral signatures of the multiple CPAs in the environment (Witter et al. 2009; Becker et al. 2009). In addition to the optical complexity of the WBLE, which creates a challenge to the application of remote sensing models, the poor performance of the standard algorithms in the lake may be attributed to the use of low pixel resolution data that can potentially cause errors related to spectral mixing and/or the use of low spectral resolution sensor data that are not optimized for detecting the CPAs, in this case specifically the chlorophyll *a*.

Current generation satellite sensors such as the Medium resolution imaging spectrometer (MERIS) are equipped with radiometric sensitivities optimized for measurements of CPAs in turbid waters. These waters normally have low reflectance due to the high absorption by water itself and its associated constituents such as phytoplankton and CDOM. MERIS has high spectral and temporal resolution (10 nm and 1–3 days, respectively) and therefore, allows for better characterization of subtle variations in spectral signals associated with the various water quality parameters.

The objective of this study was to evaluate the performance of existing published visible/NIR based empirical and semi-empirical models using reflectance data from MERIS sensor and their applicability for monitoring algal biomass in the WBLE. The algorithms were applied using MERIS bands that are sensitive to chlorophyll *a* attenuation spectral features and include: absorption features near 490 nm, minimum absorption coupled with cellular scattering near 560 nm and the red absorption features near 665 nm, and the chlorophyll *a* fluorescence peak near 680 nm.

## Data acquisition and methodology

### Field measurements

Assessment of models that predict concentrations of biogeochemical proxies requires collocated in situ data. In the

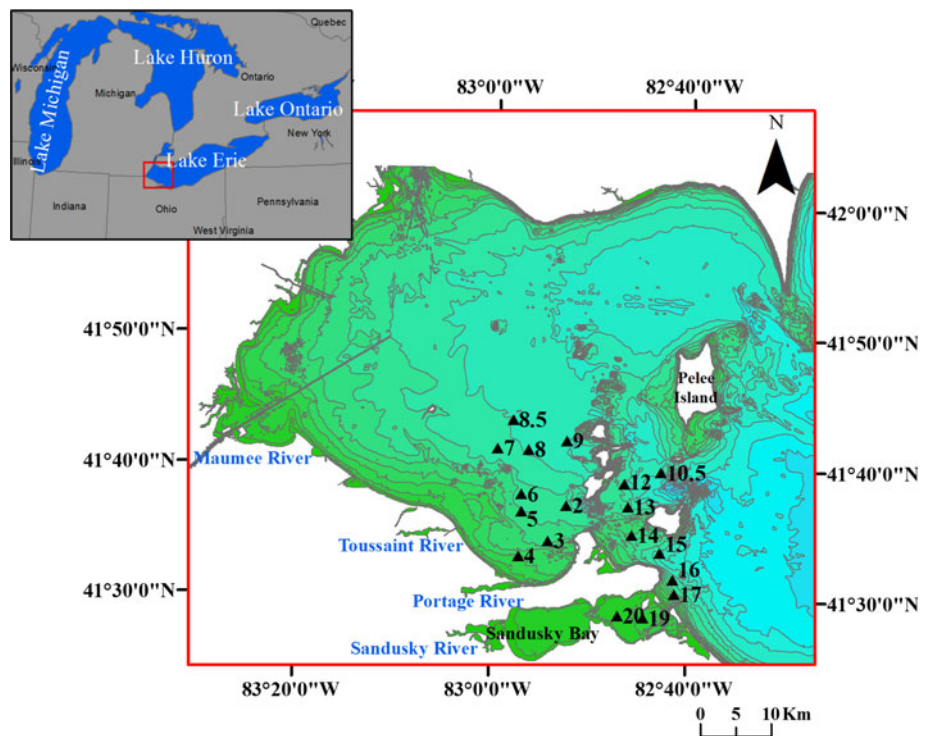
summers of 2009 and 2010, in situ data and water samples were collected from the Western Basin of Lake Erie aboard the R/V Gibraltar III or R/V Erie Monitor. These cruises were concurrent with MERIS satellite overpasses. A total of 90 observations were made by visiting 18 stations during 5 cruises over a two summer periods. Completion of each transect, which was designed to collect water samples from a variety of environments, required approximately 10 h. Sample locations were stored as waypoints in a marine GPS to verify re-occupation of the same site during each cruise. Stations were located between Sandusky Bay and Pelee Island (Fig. 1). Station locations were pre-selected to be at least 2 km away from terrestrial bodies to avoid contamination of satellite pixels by land. Water quality properties (e.g., Secchi depth, biogeochemical proxies) were measured at each station and the field campaign included collection of water samples using screw capped Nalgene bottles for laboratory analysis. A submersible HACH Hydrolab DS5X equipped with multi-parameter sonde was used to measure the chlorophyll *a*, and phycocyanin concentrations among other biogeochemical proxies such as water temperature, pH, conductivity, salinity, dissolved oxygen, although here we focus on the plant pigment data only. Absorbance of CDOM, which is indicative of its concentration, was measured in situ using UV CYCLOPS-7 submersible fluorometer. All of the sensor probes were calibrated using standards. The chlorophyll *a* sensor was calibrated by the manufacturer, HACH. Quinine sulfate was used to calibrate the Cyclops-7 CDOM fluorometer.

Satellite imagery

Five Full Resolution (FR) MERIS Level-1b images were acquired for summer of 2009 and 2010 from the European Space Agency's (ESA) data gateway. These dates were selected on the basis of the coincident field campaign for in situ data when cloud coverage conditions over the WBLE were minimal. The FR-MERIS sensor is equipped with 15 bands representing the visible/NIR spectral range with 300 m and 10 nm spatial and spectral resolutions, respectively. In this study, only bands with wavelengths between 0.4 and 0.9 μm were used. The Basic Toolbox for ENVISAT (A) ATSR and MERIS (BEAM)-4.6 visualization, analyzing and processing software developed by Brockmann-consult, Germany, was used for converting the images from Level-1b to Level-2b which includes georectification and radiometric corrections.

Digital image processing including atmospheric correction was carried out on the images to account for multiple scattering and absorption due to atmospheric constituents. Removal of atmospheric effects is crucial to reduce effects of path radiance. In turbid waters such as the WBLE, the assumption of negligible reflectance at NIR wavelength becomes invalid due to increased scattering from non-algal components. Therefore, the conventional method for image correction, the black pixel approach does not hold (Schalles 2006; Morel and Prieur 1977). Improved versions of dark pixel atmospheric corrections methods such as the NIR bands procedure (Gordon and Wang

**Fig. 1** Bathymetric map of the Western Basin of Lake Erie and the locations of 18 sampling stations visited during multiple cruises using RV Gibraltar III and Erie Monitor. The lake interacts with terrestrial environment through fluxes of the Maumee, Sandusky, Portage, Toussaint and other rivers such as the Detroit, which drain into the north western side of the basin (not shown). The inset shows, Lake Erie as part of the Great Lakes Basin



1994), the SWIR bands procedure (Wang and Shi 2005) and the Bright pixel atmospheric correction (Aiken and Moore 2000) atmospheric corrections have been developed and assessed in turbid waters (Moses et al. 2009). These methods account for absorption of water vapor in the NIR and do not make the classical assumption of zero reflectance in the NIR. However, according to Moses et al. (2009) the water-leaving radiance is very low in the NIR region and hence very sensitive to changes in the non-uniform path radiance effects. Therefore, a stable atmospheric correction, resulting in accurate retrievals of NIR reflectance, is required to the success of the models. A more stable recently developed atmospheric correction model for MERIS data is the Case 2 regional (C2R) atmospheric correction. This model is based on a neural network procedure specifically developed for turbid waters (Doerffer and Schiller 2007). It involves a two-step procedure—(a) a forward neural network for the retrieval of water-leaving radiances and, subsequently, remote sensing reflectance from the radiances, and (b) a backward neural network for the retrieval of the inherent optical properties of water and, subsequently, the concentrations of constituents by inverting the remote sensing reflectance. The neural networks are trained based on radiances simulated by radiative transfer solutions and built to parameterize the relationships between the top-of-atmosphere radiances and the water-leaving radiances (for the forward model) and between the remote sensing reflectance and the inherent optical properties (for the backward model). For this work, the recorded radiances at 12 MERIS wavebands (in visible and NIR wavelengths) are used in the neural network based atmospheric correction.

### Spectral analysis

Primary objectives of aquatic visible and near-infrared remote sensing include: identifying the optical properties of CPAs and quantifying them remotely. Radiative transfer models show the fundamental relationship that exist between remote sensing reflectance  $R(\lambda)$  and the inherent optical properties of waters—the backscattering coefficient [ $b_b(\lambda)$ ] and the absorption coefficient [ $a(\lambda)$ ] i.e.,

$$R(\lambda) = \frac{f(\lambda)}{Q(\lambda)} \frac{b_b(\lambda)}{a(\lambda) + b_b(\lambda)} \quad (1)$$

The  $f$  and  $Q$  factor represent the geometry of the light field that affects the  $R(\lambda)$

The total spectral absorption coefficient [ $a(\lambda)$ ] in  $m^{-1}$ , within the water body can be described by:

$$a(\lambda) = a_w(\lambda) + a_{ph}^*(\lambda)c_{Chl} + a_{cdom}(\lambda) + a_{SM}^*(\lambda)c_{SM} \quad (2)$$

where  $a_w(\lambda)$ ,  $a_{ph}(\lambda)$ ,  $a_{cdom}(\lambda)$  and  $a_{SM}(\lambda)$  are the absorption coefficients of pure water, phytoplankton, dissolved

organic matter and suspended matter, respectively.  $a_{bph}^*(\lambda)$  is chlorophyll-specific absorption coefficient of phytoplankton and  $a_{SM}^*(\lambda)$  is the specific spectral absorption coefficient of suspended matter. The spectral backscattering coefficient is another inherent optical property that affects the magnitude of the reflectance from water bodies (Gons 1999). The total backscattering coefficient,  $b_b(\lambda)$  with in the water body can be described by:

$$b_b(\lambda) = 0.5b_{bw}(\lambda) + b_{bph}^*(\lambda)c_{Chl} + b_{cdom}(\lambda) + b_{bSM}^*(\lambda)c_{SM} \quad (3)$$

Where  $b_{bw}(\lambda)$  is the scattering coefficient of pure water which accounts for refraction due to path transmittance between medium transitions (air–water), it is assumed that backscattering is always 50 % of total backscattering by water and therefore expressed as  $0.5b_{bw}$  (Mobley 1994). The  $b_{bph}(\lambda)$  represents the backscattering coefficient of phytoplankton and  $b_{bSM}(\lambda)$  is the backscattering coefficient of suspended matter. The degree of scattering of dissolved organic matter is negligible and assumed to be null,  $b_{cdom}(\lambda) \approx 0$ . In Eq. (3),  $b_{bph}^*(\lambda)$  is chlorophyll-specific spectral backscattering coefficient of phytoplankton and  $b_{bSM}^*(\lambda)$  is the specific backscattering coefficient of suspended matter.

Most of the existing bio-optical models that are developed for estimating chlorophyll  $a$  in aquatic environments are based on the relationship expressed in Eq. (1) (Gordon et al. 1988; El-Alem et al. 2012). The interaction of chlorophyll  $a$  and water absorption provides important insights for the interpretation of maxima and minima in the spectral reflectance curves. In Case 2 waters were multiple CPAs exist the performance of the chlorophyll  $a$  models will depend on the extent to which the absorption and backscattering effects from non-algal components ( $a_w(\lambda)$ ,  $a_{cdom}(\lambda)$  and  $a_{SM}(\lambda)$  and  $b_{bSM}(\lambda)$ ) are accounted for so that the attenuation (absorption and scattering) induced by the pigment can be isolated independently. In the WBLE, absorption due to CDOM attenuates chlorophyll  $a$  signals with absorption effects inversely proportional to wavelength (Kutser et al. 2005). Backscatter from TSM and absorption of water itself also influences the reflectance across the visible-infrared spectrum, thus affecting chlorophyll  $a$  induced signals (Bukata et al. 1994). Isolating the spectral windows that correlate with the apparent optical property of chlorophyll  $a$ , independent of other water constituents requires a robust spectral analysis technique. Bale et al. (1994) showed that increasing the concentrations of phytoplankton biomass or CDOM have no effect on the spectral shape of the reflectance near the NIR region, thus the optical signatures of materials. The NIR region can thus be used to monitor and account for the

contribution due to suspended sediments without interference from plant pigment or their degradation products.

In the WBLE, the optical properties of the multiple CPAs overlap in the visible range, and therefore the differentiation of the signatures requires the selection of optimal bands (Ali et al. 2012). In this study models that use chlorophyll *a*-sensitive spectral windows were applied using MERIS data (Fig. 2).

This study evaluated two-band algorithms based on a regionally developed blue-green model given by Witter et al. (2009) and a NIR-red model given by Moses et al. (2009) expressed as:

$$\text{chl}_a(\text{MERIS}) \propto \frac{R_{(\lambda_1)}^{-1}}{R_{(\lambda_2)}^{-1}} \quad (4)$$

These models are based on ratios of spectral regions that represent maximum absorption and minimum absorption due to chlorophyll *a*. The spectral regions are matched with the corresponding MERIS bands.

The second NIR-red based empirical model that was applied in the WBLE is given by Moses et al. (2009) and this algorithm uses three bands and has been employed in several studies (Dall’Olmo and Gitelson 2005; Moses et al. 2009; Gitelson et al. 2008; Gitelson 1992; Gurlin et al. 2011):

$$\text{chl}_a(\text{MERIS}) \propto \left( R_{(\lambda_1)}^{-1} - R_{(\lambda_2)}^{-1} \right) \times R_{(\lambda_3)}^{-1} \quad (5)$$

The NIR-red based three-band model (Eq. 5) includes a third band  $R_{(\lambda_3)}^{-1}$  as a normalizing multiplication factor to remove effects due to the backscatter. This is assumed to improve the sensitivity of the model to chlorophyll *a* variability. The multiplying factor is employed assuming that pigment and CDOM absorption is negligible near  $R_{(\lambda_3)}^{-1}$ .

Two semi-empirical models implemented in this study are given by Simis et al. (2005) (Eq. 6) and Gons (1999) (Eq. 7):

$$\text{chl}_a(\text{MERIS}) \propto \left( \left\{ \left[ \frac{R_{\lambda_1}}{R_{\lambda_2}} \right] \times \left[ R_{w708}^{-1} + b_b \right] \right\} - b_b - R_{w665}^{-1} \times \delta^{-1} \right) \quad (6)$$

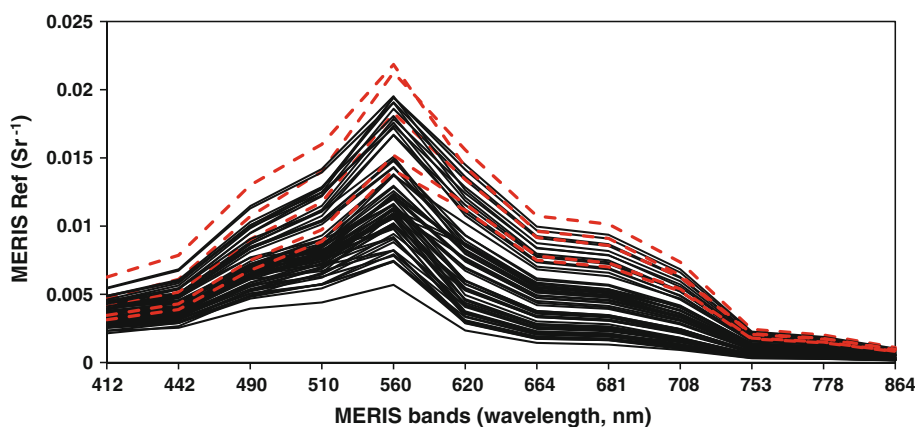
$$\text{chl}_a(\text{MERIS}) \propto \left( \left\{ \left[ \frac{R_{\lambda_1} + b_b}{R_{\lambda_2} + b_b} \right] \times \left[ R_{w708}^{-1} + b_b \right] \right\} - b_b - R_{w665}^{-1} \right) \quad (7)$$

The semi-empirical models are optimized to MERIS NIR bands that are effective to retrieve the absorption of chlorophyll *a* in the WBLE. The Gons (1999) algorithm accounts for the effect of backscattering ( $b_b$ ) and absorption due to water itself. In the present work, the backscattering coefficient was retrieved using the 775 nm band of MERIS following Gons (1999) procedure. This is a spectral region where absorption by other CPAs is assumed to be very small compared to absorption due to water (Gons 1999; Kirk 1994). In the Simis et al. (2005) algorithm, in addition to backscattering, effects due to CDOM and the accessory pigment, phycocyanin, are accounted for, using a correction factor  $\delta$ , which reflects the ratio of retrieved absorption versus measured absorption by chlorophyll *a* at NIR wavelength. For this work, the value of the correction factor  $\delta$  was taken directly from Simis et al. (2005). These parameters are appropriate for this application because they were devised for use in shallow lakes dominated by blue-green algae similar to the WBLE.

## Results and discussions

The spectral plot of the MERIS reflectance represents apparent optical properties of the water in the WBLE and clearly showed evidence of multiple CPAs (Fig. 2). The reflectance values are highly variable in the visible and NIR range. The blue-green spectral range shows reflectance patterns typically observed in turbid waters (Schalles et al. 2002) with significant absorption due to chlorophyll

**Fig. 2** Spectral plot of pixels representing 18 stations based on MERIS data after atmospheric correction was applied. *Dashed red lines* represent spectra of stations from Sandusky Bay (Stations 19 and 20). The arrows show positions of chlorophyll *a* attenuation features, including one due to phycocyanin at 620 nm, which is the major accessory pigment in the WBLE



*a*, CDOM and other associated constituents. A local reflectance maximum is observed near 560 nm, also referred to as the green peak. This is the mainly due to minimum absorption by chlorophyll *a* combined with scattering effects. The reflectance peak at the red/NIR edge, which is mainly due to fluorescence from phytoplankton, is not strongly apparent in the satellite data. The data indicates local minimum near 620 nm due to phyco-cyanin, which is the major accessory pigment in blue-green algae, a prominent algae documented in the Lake (Brittain et al. 2000). The local minimum observed near 665 nm is due to chlorophyll *a* absorption. The absorption troughs in the red region, near 620 and 665 nm and the reflectance peaks at 560 and 680 nm are more noticeable in spectra (dashed lines) from stations closer to Sandusky Bay than in the open waters of WBLE (Figs. 1, 2).

CPAs in the WBLE

The average in situ concentration of chlorophyll *a* was 5.68 and 8.07 µg/l in June and September of 2009, respectively. In September, the concentrations across the basin varied between 4.96 and 9.61 µg/l with the higher concentration values recorded at stations located in the Sandusky Bay. In summer of 2010, chlorophyll *a* concentrations in the basin ranged from 2.14 to 10.67 µg/l. The standard deviation of the chlorophyll *a* concentrations decreased from 2.71 to 0.79 µg/l between July and September, in 2010. The high standard deviation of chlorophyll *a* concentrations in July is attributed to the relatively higher seasonal algal density in the Sandusky Bay. During the early summer, river discharges are high and significant amounts of terrestrial matter, including nutrients, are dumped into Sandusky Bay. This increases the combined concentrations of

allochthonous and autochthonous phytoplankton and consequently higher chlorophyll *a* concentrations are recorded at stations located in Sandusky Bay (Stations 17, 19 and 20). This condition results in large variability of chlorophyll *a* between the waters in Sandusky Bay and the central WBLE. By late summer (September), the river discharges decrease and the waters between the two sub basins undergo mixing and the variability of chlorophyll *a* in the WBLE lowers.

Descriptive statistics of CDOM in the WBLE shows that the absorbance ranged from 0.115 to 1.38 m<sup>-1</sup>, with an average value of 0.375 m<sup>-1</sup>. This result is consistent with the findings of Binding et al. (2008) from their filtrate samples collected in Lake Erie. During July of 2010, significantly higher absorbance was recorded at stations 3, 4, 17, 19 and 20 (Fig. 3). Stations 3 and 4 are located close to the discharge zones of the Toussaint and Portage Rivers and stations 17, 19, and 20 are located in the Sandusky Bay, which is a shallow basin heavily influenced by terrestrial matters. This suggests that the optical properties of the waters near discharge zones are heavily influenced by terrestrially derived CDOM. As shown in Fig. 3, the spatial variability of CDOM concentrations across the WBLE decreases during the summer period. This may be attributed to the decreasing stream flow from late spring to summer and at the same time dispersion of in-water constituents into central WBLE.

The spatial structure of CDOM is similar to the chlorophyll *a* dynamics, providing strong evidence of the influence of rivers on the algal distributions observed in the WBLE (Fig. 4). Riverine input makes nutrients readily available for primary producers, and this increases the productivity of the lake system. Constituents such as CDOM absorb significant amount radiation in the UV-B

**Fig. 3** Spatial and temporal variability of CDOM in the WBLE during summer of 2010 based on data from in situ measurements. Missing values due to instrument errors

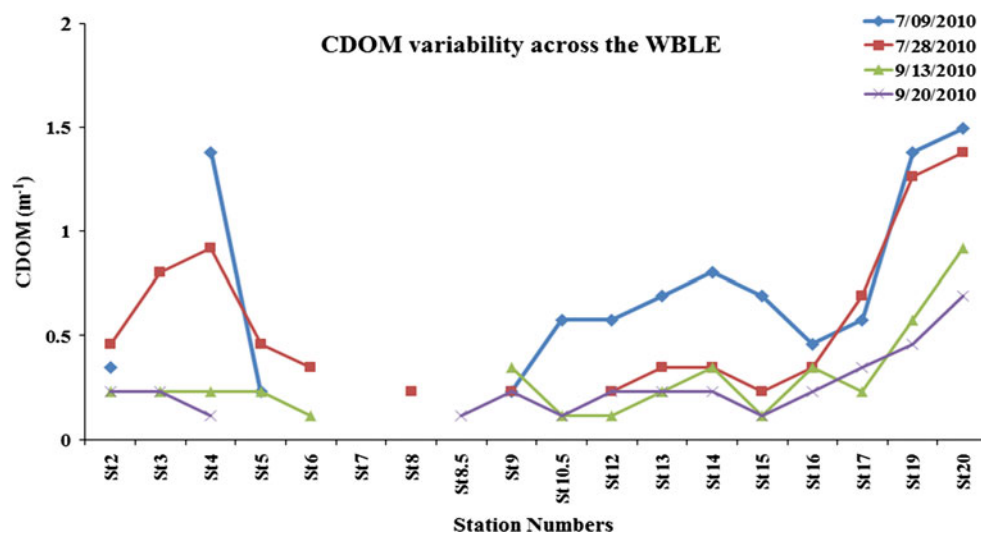
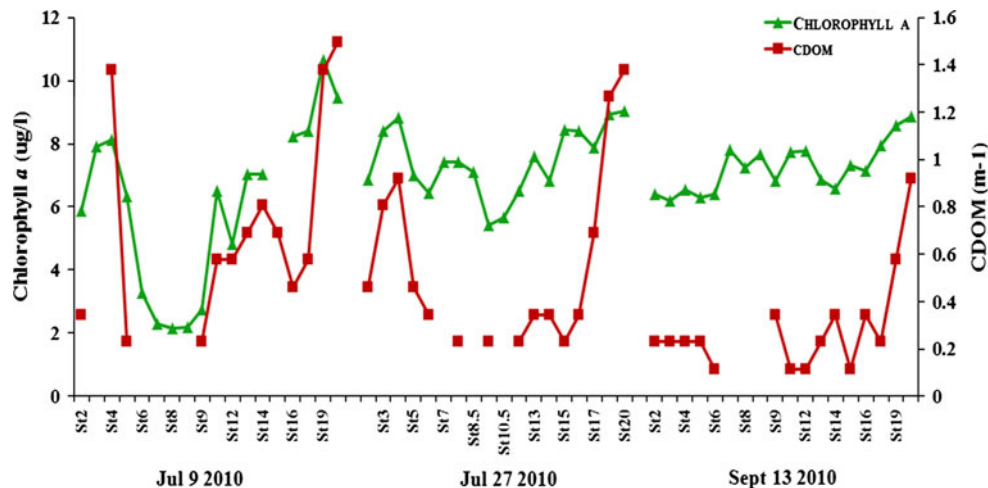


**Fig. 4** In-situ measurement of CPAs shows the variability of chlorophyll *a* and CDOM in the WBLE during summer of 2010



region, thus reducing the energy available for primary producers. This may influence the community structure of the lake system by favoring primary producers that can utilize energy in the longer wavelength region. In the WBLE, the cyanobacteria represent the dominant bio-community (Makarewicz 1993). These organisms possess accessory pigments (e.g., phycocyanin and carotene) allowing them to harvest radiant energy beyond the blue spectral region and making their productivity less sensitive to the presence of CDOM.

Away from the littoral zone, in the central WBLE, CDOM concentration is relatively low and the influence of rivers is reduced. A different bio-community structure makes up the biomass. Studies by Ali et al. (2012) have indicated that the blue-green algae are generally lower in central WBLE than in Sandusky Bay, suggesting that this assemblage is more important in the Sandusky Bay than in central WBLE. The study has further indicated that central WBLE is dominated by the diatom/green algae community, which is consistent with the concept of CDOM interference.

**Chlorophyll *a* prediction**

*Empirical models*

Band ratios such as  $R_{443}/R_{565}$  and  $R_{520}/R_{565}$  were commonly used to estimate chlorophyll *a* in ocean waters (Arnone et al. 2006; Morel and Prieur, 1977). However, O'Reilly et al. (1998) and other studies have clearly indicated that blue-green models did not perform well in Case 2 waters due to the presence of multiple constituents (CDOM, suspended matters) affecting the absorption characteristics of the Soret bands. Witter et al. (2009) developed a regional blue-green chlorophyll *a* algorithm (Eq. 8) based on co-located satellite observations and field-collected samples from the WBLE.

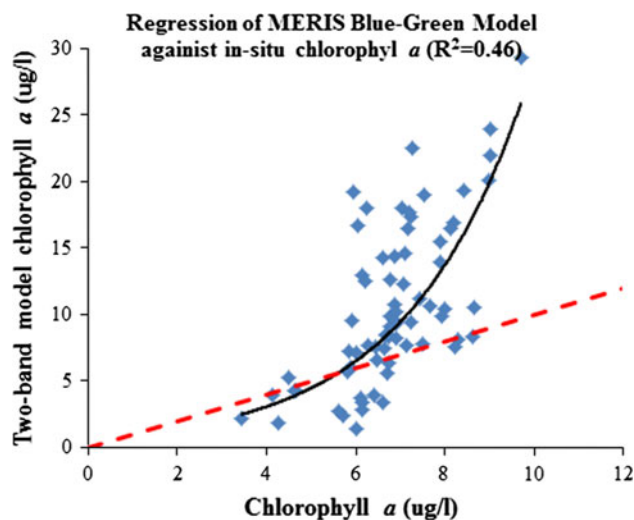


**Fig. 5** Regression plot of MERIS based blue-green chlorophyll *a* model versus in situ chlorophyll *a* concentrations

$$chl\_a_{(MERIS)} \propto \frac{R_{490}^{-1}}{R_{560}^{-1}} \tag{8}$$

This algorithm was applied in this study using MERIS data from 2009 and 2010 and the result is illustrated in Fig. 5. The regional algorithm gave  $R^2$  values of 0.46 and indicated that the blue-green algorithm overestimates the chlorophyll *a* values in the WBLE. Careful examination of the results indicates that for the low chlorophyll *a* concentrations (<6  $\mu\text{g/l}$ ), the predicted values plot closer to the 1:1 line, but with higher chlorophyll *a* concentrations the model overestimates chlorophyll *a* values showing exponential relationship with the field measurements. The bias towards high values corresponds to samples collected from stations that are closer to river discharge zone or in areas where Secchi depth was low (Stations 3 4, 17, 19, 20). The overestimation is due to optical interference from other in-water constituents such

as CDOM that is not necessarily correlated with pigment concentration.

MERIS is equipped with chlorophyll *a* red absorption band (665 nm) and a narrow NIR band (708, 7.5 nm band width) which is sensitive to non-algal absorption. Regression analysis between a two-band red/NIR (Eq. 9) MERIS based model (Moses et al. 2009) and chlorophyll *a* concentration for the WBLE is shown in Fig. 6a. The MERIS-based two-band model is able to explain approximately 60 % of the chlorophyll *a* variability in the WBLE. The band ratioing removed effects of other non-algal in-water constituents, and therefore the magnitude of the model increases proportionally with chlorophyll *a* concentration. Application of band ratios also removes systematic errors from instrumental disturbances and minimizes effects due

to path radiance especially when working in smaller area where atmospheric effects can be assumed to be uniform (Binding et al. 2008; Gilerson et al. 2010; Babin et al. 2000; Sokoletsky et al. 2011). Another important strength of the two-band ratio model is its capability to remove back-scattering effects. However, scattering effects can significantly deteriorate the performance of the model. In this case, some of the factors that may have limited the performance of the two-band red/NIR model are absorption effects of accessory pigments, e.g., phycocyanin, and absorption due to the dissolved organic matter which varies as a function of ( $\lambda^{-1}$ ).

$$\text{chl}_a(\text{MERIS}) \propto \frac{R_{665}^{-1}}{R_{708}^{-1}} \tag{9}$$

Regression analysis of a three-band MERIS model based using  $R_{665}$ ,  $R_{708}$  and  $R_{753}$  versus chlorophyll *a* gave  $R^2$  value of 0.57, indicating that this model has some potential for explaining chlorophyll *a* variability in the turbid WBLE. Model performance is illustrated using regression analysis (Fig. 6b). The  $R^2$  values obtained from the MERIS based three-band model (Eq. 10) is relatively low and this can be generally attributed to the absorption effects of water on the longer wavelengths ( $>720$  nm).

$$\text{chl}_a(\text{MERIS}) \propto \frac{(R_{665}^{-1} - R_{708}^{-1})}{R_{753}^{-1}} \tag{10}$$

In comparison to the two-band model, the performance of the three-band model is lower. This is because firstly, with increasing wavelength ranging from 665 to 708 nm, the absorption of water exponentially increases due to the low energy incident photons being easily attenuated (Babin et al. 2000). This in turn reduces reflectance from scattering effects of suspended particles and therefore subtracting absorption effects between the red and the NIR bands may not effectively remove the effects of backscattering causing the relationship between the model derived chlorophyll *a* estimate and in situ chlorophyll *a* to be relatively low. A second potential contribution to errors in the three-band prediction model of chlorophyll *a* is due to the use of  $R_{753}$  in the model. This band is a multiplication factor that is usually applied to account for the backscattering from inorganic matters. However, in aquatic bodies, the irradiance of water at this wavelength region produces very low reflectance values and this low values are easily influenced by effects of path radiance and are also more susceptible to stochastic errors (Babin et al. 2000; Sokoletsky et al. 2011).

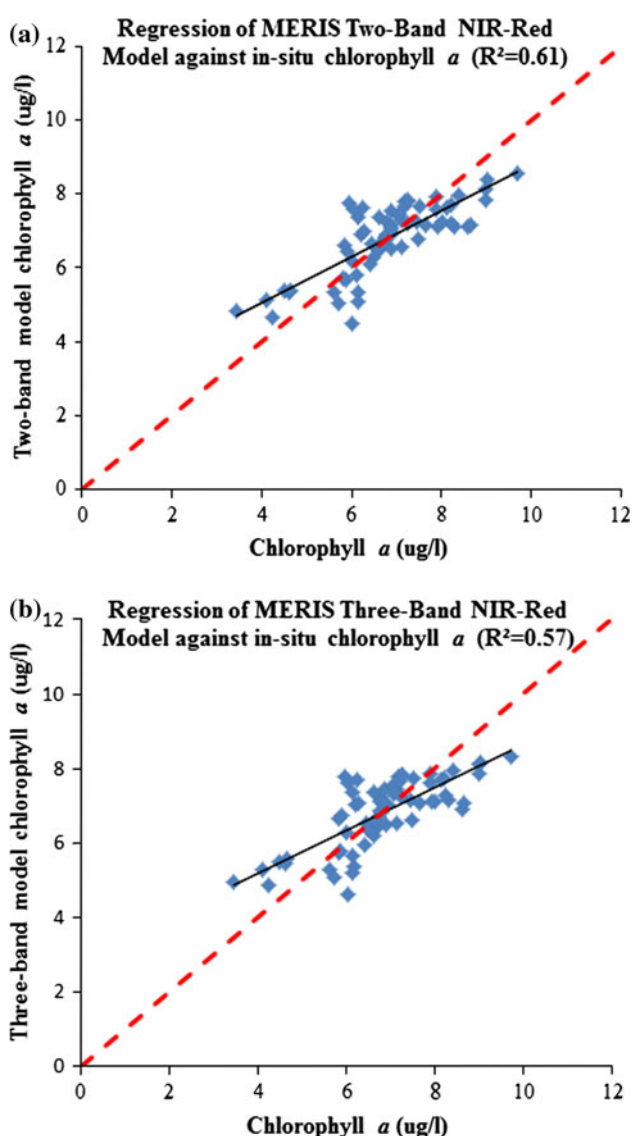


**Fig. 6** Regression plot of MERIS based chlorophyll *a* models versus the chlorophyll *a* concentrations measured in situ **a** two-band red/NIR and **b** three-band red/NIR chlorophyll *a* model

*Semi-analytical models*

Semi-analytical models constitute another approach for estimating chlorophyll *a* from satellite sensors. These models are based on known spectral features that are

discovered from the correlation between the apparent optical properties (AOPs) and the inherent optical properties (IOPs) of the water (Gordon and Wang, 1994). In Case 2 waters, most of the semi-analytical algorithms used to retrieve chlorophyll *a* utilize the red and near-infrared (NIR) spectral region (650–750 nm) (Gons 1999; Simis et al. 2005).

The relationship between the Simis et al. (2005) NIR/red based model (Eq. 11) and in situ chlorophyll *a* concentration is stronger, with a coefficient of determination of 0.65. Figure 7a shows a plot of the Simis et al. (2005) model versus observed chlorophyll *a* concentrations. The best fit line is relatively close to the 1:1 line, indicating the potential of the Simis et al. (2005) model in retrieving CPAs. The higher predictive power of the model is attributed to the incorporation of correction factors such as absorption effects due to pure water ( $a_w$ ), backscatter ( $b_b$ ) from suspended matter and interference due to phycocyanin ( $\delta^{-1}$ ). The relatively higher  $R^2$  value clearly indicates

the importance of accounting for optical interference of other in-water constituents such as phycocyanin and suspended matter on the chlorophyll *a* reflectance.

$$\text{chl}_a(\text{MERIS}) \propto \left( \left\{ \left[ \frac{R_{708}}{R_{665}} \right] \times \left[ R_{w708}^{-1} + b_b \right] \right\} - b_b - R_{w665}^{-1} \times \delta^{-1} \right) \tag{11}$$

Although it is demonstrated that the Simis et al. (2005) model performs well in the retrieval of chlorophyll *a* in a wide range of eutrophic lakes (Simis et al. 2005; Novoa et al. 2012; Gurlin 2012), the predictive power of the model can further be improved by optimizing correction factors such as  $\delta$  based on local measurements of pigment specific absorption. This will provide an opportunity to correct for any offset values due to absorption by tripton and CDOM, which are significant water quality parameters in the WBLE (Makarewicz 1993). The Simis et al. (2005) model only corrects for the absorption effects due to phycocyanin using correction factors derived from slope of a line constructed between the measured absorption values of phytoplankton and total absorption at 665 nm. Generally, the model ignores the offsets values due to CDOM and tripton assuming it to be negligible near the red/NIR region and does not subtract it from the computed chlorophyll *a* absorption.

The second semi-analytical applied to the WBLE is the red/NIR model (Eq. 12) developed by Gons (1999). This model is very similar to the Simis et al. (2005) model, except that the model does not account for absorption by accessory pigments.

$$\text{chl}_a(\text{MERIS}) \propto \left( \left\{ \left[ \frac{R_{708} + b_b}{R_{665} + b_b} \right] \times \left[ R_{w708}^{-1} + b_b \right] \right\} - b_b - R_{w665}^{-1} \right) \tag{12}$$

Plots of Gons (1999) red/NIR based chlorophyll *a* estimate versus in situ chlorophyll *a* concentrations show coefficient of determination of 0.61 (Fig. 7b). Relative to the Simis et al. (2005) algorithm, the Gons (1999) model gave lower prediction accuracy with very flat best fit line. This is mainly due to simplified assumptions taken in the development of the model. These include the assumption of negligible pigment reflectance in the NIR region. In addition, absorption by CDOM and tripton in the red/NIR is not accounted for in the model.

The Gons (1999) model overestimates low to moderate chlorophyll *a* concentrations, and tends to underestimate the higher chlorophyll *a* concentrations (Fig. 7b). The simplified assumption of negligible absorption of pigment in the NIR region leads to overestimation by the reflectance in the red region (665 nm) and therefore lower ratio between 708 and 665 nm, causing underestimation of chlorophyll *a* concentrations. Similarly, the assumption of the zero-absorption effects of CDOM and tripton may

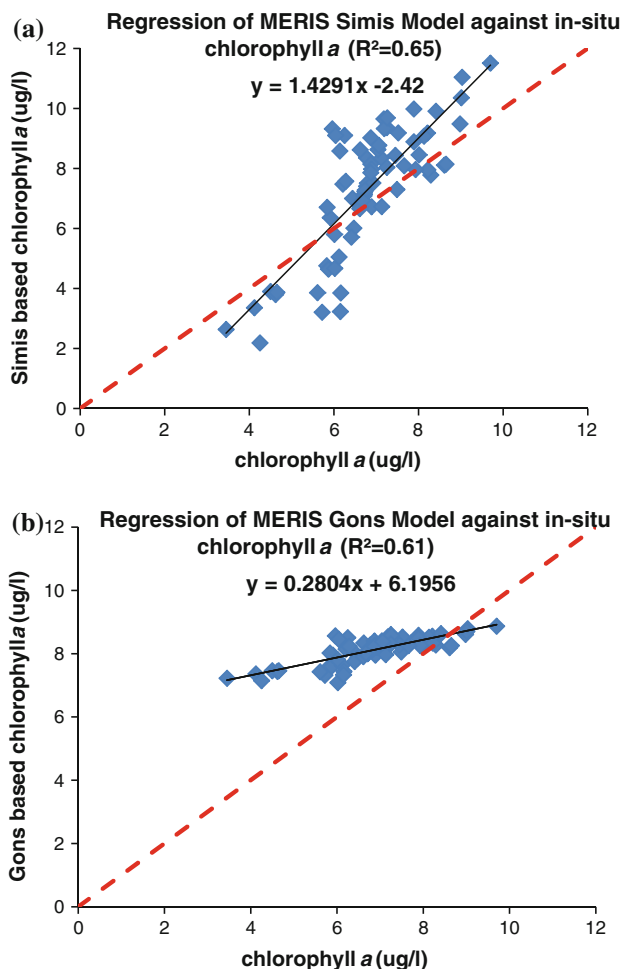


**Fig. 7** Regression plot of MERIS based chlorophyll *a* model versus the chlorophyll *a* concentrations measured in situ **a** Simis et al. (2005), red/NIR and **b** Gons (1999), red/NIR chlorophyll *a* model

cause an underestimation of reflectance in the red region (lower  $R_{708}/R_{665}$  ratio), which may not necessarily be correlated with chlorophyll  $a$  concentration. This leads to erroneous prediction of higher chlorophyll  $a$ .

#### Calibration-validation of chlorophyll $a$ algorithms

The two-band (Moses et al. 2009) and the semi-empirical algorithms (Gons 1999; Simis et al. 2005) have produced the best results among the different empirical and semi-empirical chlorophyll  $a$  algorithms, with  $R^2$  of 0.61, 0.61 and 0.65, respectively. The performance the three models were further evaluated using the leave-one-out cross-validation method (Kohavi 1995). All three models indicate statistically significant ( $p < 0.05$ )  $R^2$ -PRED values which indicates the efficiency of the models to predict responses for new observations. The RMSE of the predicted values are comparable to the error values of the fitting models. The Simis et al. (2005) model with relatively lower RMSE-PRED and higher  $R^2$ -PRED values shows slightly greater predictive ability when applied to the WBLE environment as compared to the Gons (1999) and the two-band Moses et al. (2009) algorithm (Table 1).

#### Uncertainties

The algorithms presented in this work illustrate the strength of the red/NIR and blue-green based bio-optical models in detecting the variability of chlorophyll  $a$  when applied to high resolution satellite data (MERIS) in turbid waters such as the WBLE. However, studies indicated that the performance of the satellite algorithm comes with certain uncertainties. The models are not stable and calibration work has always been difficult due to various assumptions and physical factors (Moses et al. 2009; Kutser et al. 2005; Gitelson et al. 2008; Simis et al. 2005). Several factors limit the potential of satellite algorithms to estimate the concentrations of in-water constituents.

#### Assumption of negligible effects due to other components

In Case 2 waters, the red/NIR spectral range is often used to develop algorithms that estimate pigment concentration

**Table 1** Summary of calibration-validation of chlorophyll  $a$  algorithms based on Simis et al. (2005), Gons (1999) and two-band Moses et al. (2009)

Models	$N$	RMSE	$R^2$	RMSE-PRED	$R^2$ -PRED
Simis	71	0.71	0.65	0.73	0.63
Gons	71	0.75	0.61	0.77	0.59
Moses	71	0.74	0.61	0.76	0.59

in the water column. The red-edge of the spectrum is usually invoked in order to minimize the complicating influences of other in-water constituents such as CDOM and inorganic particles. However, assumption of negligible effects of CDOM and inorganic particles in the red/NIR models led to significant bias.

#### Temporal variability

Data collected using conventional in situ methods cannot sample multiple water points at the same time. However, a satellite has the capability to capture optical properties of large inland water bodies instantly. The time difference between the sampling period and the satellite data may be enough to have significant changes in the optical properties of the water, especially in shallow-turbid waters such as the WBLE. Instant wind action over the waters of WBLE causes mixing, significantly changing the optical and hydrochemical properties of the water column. The small difference in the time of data acquisition can introduces random errors that significantly reduce the correlation factor between the retrieved constituents from the two platforms hence degrading model performance.

#### Pixel heterogeneity

Although in this study, higher spatial resolution satellite data were used compared to previous studies, in optically complex aquatic systems such as in the WBLE, the spatial variability of in-water constituents may be large. The spatial resolutions ( $0.09 \text{ km}^2$  for MERIS) may be too coarse to correlate with in situ point measurements. In such cases collocated in situ data may not represent conditions averaged over the satellite pixel. This can reduce the correlation between the in situ measurements and the satellite retrievals.

#### Path radiance correction

The influence of path radiance due to atmospheric scattering can be substantial and the success of satellite remote sensing in predicting water quality parameters depends on the accuracy of the applied atmospheric correction module. Several atmospheric correction procedures including the NIR bands procedure (Gordon and Wang 1994), the SWIR bands procedure (Wang and Shi 2005), Bright pixel atmospheric correction (Aiken and Moore 2000) and the Case 2 regional processor (Doerffer and Schiller 2007) have been tested to correct for path radiance. The Case 2 waters regional algorithm has been selected as the optimal models. However, without synchronized in situ measurements of water-leaving radiances, it is not possible to assess accuracy of the procedures from the reflectance

curves. Implementing accurate corrections due to interference of atmospheric constituents remains a significant challenge within optical remote sensing.

### Conclusion

The results have illustrated the potential of the remote sensing algorithms utilizing high resolution MERIS data in red/NIR wavelength region to estimate chlorophyll *a* concentrations in optically complex productive waters. Among the various models applied, results indicate that the Simis et al. (2005) algorithm provides the best estimates of chlorophyll *a* in the optically complex waters of the WBLE. The Simis algorithm accounts for back scattering effects and the absorption effects due to major accessory pigment, phycocyanin. These corrections significantly increased its performance relative to others, such as the Gons (1999) model which does not account for effects of phycocyanin. The addition of correction factors for other optically active constituents including suspended sediments and CDOM will improve model performance and the task of formulating the correction factors is a promising direction for future research.

The increased spatial and spectral resolution of the FR-MERIS sensor aboard Envisat along with its chlorophyll *a*-sensitive bands such as 665 nm significantly increased the effectiveness of satellite-based remote sensing to estimate chlorophyll *a* distributions and hence the effective monitoring of water quality in large water bodies such as the WBLE. To develop more robust bio-optical models, future efforts must focus on: (a) improving atmospheric correction methods through calibration-validation techniques, (b) designing better field methods to accommodate for the temporal difference and effects of ground resolution between in situ and satellite data, and (c) applying mathematical transformation techniques on full spectral information instead of narrow individual bands signatures. This will enhance retrievals of CPAs from satellite-based sensors and improve model stability.

**Acknowledgments** This research was supported by the NOAA-Ohio Sea Grant Program Grant R/ER-100-PD. Authors are thankful to Matt Thomas, Captain of the Stone Laboratory research vessels, and the Stone Laboratories, for access and research vessels required to collect the samples.

### References

Aiken J, Moore G (2000) ATBD Case 2 s bright pixel atmospheric correction. POTN-MEL-GS-0005, Center for Coastal & Marine Sciences, Plymouth Marine Laboratory, UK, p 14  
 Ali KA, Witter DL, Ortiz JD (2012) Multivariate approach to estimate color producing agents in Case 2 waters using first-derivative

spectrophotometer data. Geocarto International Taylor Francis. doi:10.1080/10106049.2012.743601  
 Babin M, Berthon J, Kopelevich OV, Campbell JW (2000) Remote sensing of Ocean colour in coastal, and other optically-complex waters. Reports of the International Ocean-Colour Coordination Group, IOCCG, Dartmouth, NS, Canada, Rep. 3  
 Babin M, Stramski D, Ferrari GM, Claustre H, Bricaud A, Obolensky G (2003) Variations in the light absorption coefficients of phytoplankton, non-algal particles, and dissolved organic matter in coastal waters around Europe. *J Geophys Res* 108(C7):3211–3230  
 Bale AJ, Tocher MD, Weaver R, Hudson SJ, Aiken J (1994) Laboratory measurements of the spectral properties of estuarine suspended particles. *Aquat Ecol* 28(3):237–244  
 Becker R, Sultan MI, Boyer GL, Twiss MR, Konopko E (2009) Mapping cyanobacterial blooms in the Great Lakes using MODIS. *J Great Lakes Res* 35:447–453. doi:10.1016/j.jglr.2009.05.007  
 Binding CE, Jerome JH, Bukata RP, Booty WG (2008) Spectral absorption properties of dissolved and particulate matter in Lake Erie. *Remote Sens Environ* 112(4):1702–1711  
 Brittain SM, Wang JL, Babcock J et al (2000) Isolation and characterization of microcystins, cyclic heptapeptide hepatotoxins from a Lake Erie strain of *Microcystis aeruginosa*. *J Great Lakes Res* 26(3):241–249  
 Bukata RP, Jerome JH, Kondratyev KY, Pozdnyakov DV (1994) Optical properties and remote sensing of inland and coastal waters. CRC Press, Boca Raton 362  
 Dall’Olmo G, Gitelson AA (2005) Effect of bio-optical parameter variability on the remote estimation of chlorophyll-*a* concentration in turbid productive waters: experimental results. *Appl Opt* 44(3):412–422  
 Dekker AG (1993) Detection of optical water quality parameters for eutrophic waters by high resolution remote sensing. Amsterdam Free Universiteit. <http://en.scientificcommons.org/34398616>  
 Dekker AG, Hoogenboom HJ, Goddijn LM, Malthus TJM (1997) The relation between inherent optical properties and reflectance spectra in turbid inland waters. *Remote Sens Rev* 15(1):59–74  
 Doerffer R, Fischer J (1994) Concentrations of chlorophyll, suspended matter and gelbstoff in case II waters derived from satellite coastal zone color scanner data with inverse modeling methods. *J Geophys Res* 99(C4):7457–7466  
 Doerffer R, Schiller H (2007) The MERIS case 2 water algorithms. *Int J Remote Sens* 28(3):517–535  
 Arnone R, Babin M, Dowell, MD, Barnard AH, Lee S, Cannizzaro JP, Berthon JF, Kopelevich OV, Campbell JW (2006) Remote sensing of inherent optical properties: fundamentals, test of algorithms, and applications. Reports of the International Ocean-Color Coordination Group No 5  
 El-Alem A, Chokmani K, Laurion I, El-Adlouni SE (2012) Comparative analysis of four models to estimate chlorophyll-*a* concentration in Case-2 waters using MODerate resolution imaging spectroradiometer (MODIS) imagery. *Remote Sens* 4(8):2373–2400. doi:10.3390/rs4082373  
 Gilerson AA, Gitelson AA, Zhou J, Gurlin D, Moses WJ, Ioannou I, Ahmed SA (2010) “Algorithms for remote estimation of chlorophyll-*a* in coastal and inland waters using red and near infrared bands”. *Natural Resour Paper* 286. <http://digitalcommons.unl.edu/natrespapers/286>  
 Gitelson A (1992) The peak near 700 nm on radiance spectra of algae and water: relationships of its magnitude and position with chlorophyll concentration. *Int J Remote Sens* 13(17):3367–3373  
 Gitelson AA, Yacobi YZ, Schalles JF, Rundquist DC, Han L, Stark R (2000) Remote estimation of phytoplankton density in productive waters. *Arch Hydrobiol Spec Issues Adv Limnol* 55:121–136

- Gitelson AA, Schalles JF, Hladik CM (2007) Remote chlorophyll-*a* retrieval in turbid, productive estuaries: Chesapeake Bay case study. *Remote Sens Environ* 109(4):464–472
- Gitelson AA, Dall'Olmo G, Moses W, Rundquist DC, Barrow T, Fisher TRA (2008) Simple semi-analytical model for remote estimation of chlorophyll-*a* in turbid waters: validation. *Remote Sens Environ* 112(9):3582–3593
- Gons HJ (1999) Optical teledetection of chlorophyll *a* in turbid inland waters. *Environ Sci Technol* 33(7):1127–1132
- Gons HJ, Rijkeboer M, Ruddick KGA (2002) Chlorophyll-retrieval algorithm for satellite imagery (medium resolution imaging spectrometer) of inland and coastal waters. *J Plankton Res* 24(9):22–947
- Gordon HR, Morel AY (1983) Remote assessment of ocean color for interpretation of satellite visible imagery: a review. Springer-Verlag, New York 114
- Gordon HR, Wang M (1994) Retrieval of water-leaving radiance and aerosol optical thickness over the oceans with SeaWiFS: a preliminary algorithm. *Appl Opt* 33(3):443–452
- Gordon HR, Brown OB, Evans RH, Brown JW, Smith RC, Baker KS (1988) A semi-analytic radiance model of ocean color. *J Geophys Res* 93(D9):10909–10924
- Gower JFR, Doerffer R, Borstad GA (1999) Interpretation of the 685 nm peak in water-leaving radiance spectra in terms of fluorescence, absorption and scattering, and its observation by MERIS. *Int J Remote Sens* 20(9):1771–1786
- Gurlin D (2012) Near infrared-red models for the remote estimation of chlorophyll- $\alpha$  concentration in optically complex turbid productive waters: from in situ measurements to aerial imagery. Dissertations and Theses in Natural Resources, Paper 46. <http://digitalcommons.unl.edu/natresdiss/46>
- Gurlin D, Gitelson AA, Moses JW (2011) Remote estimation of chl-*a* concentration in turbid productive waters—return to a simple two-band NIR-red model? *Remote Sens Environ* 115:3479–3490
- Kirk JT (1994) Light and photosynthesis in aquatic ecosystems. University Press Cambridge, UK, p 401
- Kohavi R (1995) A study of cross-validation and bootstrap for accuracy estimation and model selection. In: Proceedings of the Fourteenth International Joint Conference on Artificial Intelligence, pp 1137–1143. <http://robotics.stanford.edu/~ronnyk>
- Kutser T, Pierson DC, Kallio KY, Reinart A, Sobek S (2005) Mapping Lake CDOM by satellite remote sensing. *Remote Sens Environ* 94(4):535–540
- Makarewicz JC (1993) Phytoplankton biomass and species composition in Lake Erie, 1970 to 1987. *J Great Lakes Res* 19(2):258–274
- Martin S (2004) An introduction to ocean remote sensing. Cambridge University Press, Cambridge, p 46
- Matthews MW, Bernard S, Winter K (2010) Remote sensing of cyanobacteria-dominant algal blooms and water quality parameters in Zeekoevlei, a small hypertrophic lake, using MERIS. *Remote Sens Environ* 114(9):2070–2087
- McClain CRA (2009) Decade of satellite ocean color observations. *Annu Rev Marine Sci* 1:19–42
- Mobley CD (1994) Light and water: radiative transfer in natural waters. Academic press, San Diego
- Morel A, Prieur L (1977) Analysis of variations in ocean color. *Limnol Oceanogr* 22(4):709–722
- Moses WJ, Gitelson AA, Berdnikov S, Povazhnyy V (2009) Estimation of chlorophyll-*a* concentration in case II waters using MODIS and MERIS data—successes and challenges. *Environ Res Lett* 4:045005
- National Oceanic and Atmospheric Administration (NOAA) (2011) Experimental Lake Erie harmful algal bloom bulletin. 6
- Novoa S, Chust G, Froidefond JM, Petus C, Franco J, Orive E, Seoane S, Borja A (2012) Water quality monitoring in Basque coastal areas using local chlorophyll-*a* algorithm and MERIS images. *J Appl Remote Sens* 6(1):063519
- O'Reilly JE, Maritorena S, Mitchell BG, Siegel DA, Carder KL, Garver SA (1998) Ocean color chlorophyll algorithms for SeaWiFS. *J Geophys Res* 103(C11):24937–24953
- Ouellette AJA, Handy SM, Wilhelm SW (2006) Toxic microcystis is widespread in Lake Erie: pCR detection of toxin genes and molecular characterization of associated cyanobacterial communities. *Microb Ecol* 51(2):154–165
- Schalles JF (2006) Optical remote sensing techniques to estimate phytoplankton chlorophyll *a* concentrations in coastal waters with varying suspended matter and CDOM concentrations. In: Richardson LL, LeDrew EF (eds) Remote sensing of aquatic coastal ecosystem processes. Springer Netherlands, pp 27–79
- Schalles JF, Rundquist DC, Schiebe FR (2002) The influence of suspended clays on phytoplankton reflectance signatures and the remote estimation of chlorophyll. *Verh Int Ver Theor Angew Limnol/Proc Int Assoc Theor Appl Limnol/Trav Assoc Int Limnol Theor Appl* 27(6):3619–3625
- Simis SGH, Peters SWM, Gons HJ (2005) Remote sensing of the cyanobacterial pigment phycocyanin in turbid inland water. *Limnol Oceanogr* 50(1):237–245
- Sokoletsky LG, Ross SL, Wetz MS, Paerl HW (2011) MERIS retrieval of water quality components in the turbid Albemarle-Pamlico Sound Estuary, USA. *Remote Sens* 3:684–707. doi:10.3390/rs3040684
- Wang MH, Shi W (2005) Estimation of ocean contribution at the MODIS near-infrared wavelengths along the east coast of the US: two case studies. *Geophys Res Lett* 32:L13606
- Wang F, Zhou B, Xu JM (2009) Application of neural network and MODIS 250 m imagery for estimating suspended sediments concentration in Hangzhou Bay, China. *Environ Geol* 56:1093–1101
- Whitlock CH, Poole LR, Usry JW, Houghton WM, Witte WG, Morris WD, Gurganus EA (1981) Comparison of reflectance with backscatter and absorption parameters for turbid waters. *Appl Opt* 20:517–522
- Witter DL, Ortiz JD, Palm S, Heath RT, Budd JW (2009) Assessing the application of SeaWiFS Ocean color algorithms to Lake Erie. *J Great Lakes Res* 35(3):361–370
- Wong MS, Nichol JE, Lee KH, Emerson N (2008) Modeling water quality using Terra/MODIS 500 m satellite images. In: Proceedings of XXIIst ISPRS Congress, Vol XXXVII, pp 679–684
- Woodruff DL, Stumpf RP, Scope JA, Paerl HW (1999) Remote estimation of water clarity in optically complex estuarine waters. *Remote Sens Environ* 68:41–52